Application of Plasma and UV/H_2O_2 for the Removal of Pharmaceuticals in Synthetic Urine

Enrique E. Rodriguez[a], William A. Tarpeh[b], Krista R. Wigginton[a], and Nancy G. Love[a#]

[a]Civil and Environmental Engineering, University of Michigan, Ann Arbor, MI, United States

[b]Chemical Engineering, Stanford University, Stanford, CA, United States

Main text word count: 4139

Abstract word count: 183

[#]Address correspondence to Nancy G. Love, nglove@umich.edu, 734-763-9664

Abstract

Removal of pharmaceuticals in source-separated urine is an important step toward gaining acceptance of urine-derived fertilizers. Advanced oxidation processes (AOPs) have been studied for the removal of pharmaceuticals in various complex matrices, such as treated wastewaters. AOP methods that rely primarily on hydroxyl radicals as the oxidizing agents suffer from the impacts of scavengers. Here, we compared the performance of a dielectric barrier discharge plasma jet to ultraviolet (UV)/AOP in oxidizing six pharmaceuticals (acetaminophen, atenolol, 17α-ethynyl estradiol, ibuprofen, naproxen, and sulfamethoxazole). The results show that the plasma reactor used produced hydroxyl radicals as the primary oxidizing agent and that other oxidizing factors were minimal. Both plasma and UV/H_2O_2 experienced scavenging in fresh and hydrolyzed urine. The scavenging impacts were consistent across fresh and hydrolyzed urine for plasma whereas UV/H_2O_2 experienced greater scavenging in fresh urine. The energy required per order of magnitude of pharmaceutical transformed was up to 3 orders of magnitude lower for UV/H_2O_2 than for plasma and depended upon the matrix. Therefore, plasma can oxidize pharmaceuticals in fresh and hydrolyzed urine, and would be most useful for on-site or building-scale applications.

Introduction

Water Resource Recovery Facilities (WRRFs) invest heavily in advanced nutrient removal methods to mitigate the risks of eutrophication in surface waters, recycle nutrients,(1,2) and combat the threat of dwindling global phosphorus reserves.(3) Urine contains most of the nitrogen and phosphorus in domestic wastewater while composing less than 1% of the total volume.(4) It can be processed centrally or at the point of collection using building-scale systems(5). Separating urine at the point of generation and forming urine-derived fertilizers is a means of offsetting the energy and capital costs of nutrient removal at WRRFs(6) and of providing a concentrated, renewable stream of nutrients. Source-separated urine also produces a concentrated waste stream of pharmaceuticals that conventional wastewater treatment systems fail to fully address.(7)

Pharmaceuticals are important contaminants of concern because of their persistence in conventional wastewater treatment systems.(8) Among the options for removing pharmaceuticals, sorption-based processes and advanced oxidation processes (AOPs) are among the most common.(9–11) Several studies have been published on the treatment of pharmaceuticals in a variety of matrices by traditional AOPs like UV/H_2O_2 and UV/ozone.(12–15) These AOP methods rely upon the high oxidative potential of hydroxyl radicals to degrade micropollutants.(16) Hydroxyl radicals often have second order rate constants with organic compounds that are near the limit of diffusion, meaning they will degrade these compounds nearly as rapidly as they collide.(17) However, the broad range of chemicals that hydroxyl radicals are able to rapidly degrade limits the selectivity of hydroxyl-radical-based AOPs.(18) Reactive chemicals outside of the contaminants targeted for degradation (i.e. scavengers) limit the ability of AOP treatments to degrade target pharmaceuticals and diminishes treatment efficiency.

Plasma is an alternative method to traditional AOPs that generates oxidative radicals and other oxidative species. Previous studies have shown that UV, H_2O_2, O_3, H_2, O_2^-, and several other reactive chemical species are formed by plasma.(19–23) The generation of these species depends heavily on a wide set of factors that include (among others): reactor geometry, carrier gas, gas flow rate, type of power supply, frequency, voltage rise time, and liquid conductivity.(24–26) The potential for capturing the synergistic effects of multiple reactive chemical species makes plasma an appealing technology compared to traditional AOPs, which may not be suitable in complex matrixes such as urine. Similar to other AOPs, plasma can also provide multiple treatment benefits by serving as a disinfectant(27) and stabilizing ammonium by oxidizing it to nitrate.(28) This would be beneficial for processing source-separated urine where micropollutant elimination, pathogen disinfection, and nutrient stabilization are major priorities for fertilizer production. However, several questions need to be answered to understand the full potential of plasma for treating urine. Studies that probe plasma as a water purification method commonly rely on dyes as a proxy for micropollutants to investigate the performance of plasmas.(29–32) Consequently, the efficiency for degrading micropollutants in different matrices is largely unknown. Furthermore, it is unclear if radicals and oxidative species other than hydroxyl radical play significant roles in degrading compounds during plasma treatment.

Although there are multiple unit treatment processes for converting urine into useful products, management of pharmaceuticals in urine is understudied compared to nutrient recover for urine treatment. This study aims to assess the performance of a traditional AOP (UV/H_2O_2) and plasma AOP for oxidizing pharmaceuticals in fresh or hydrolyzed urine. To evaluate plasma, we apply a dielectric barrier discharge plasma reactor in liquid using laboratory studies with a suite of pharmaceutical compounds rather than dyes. The kinetic rate of pharmaceutical loss by both

AOP methods is determined and the likely oxidative mechanism responsible for degradation is assessed. Finally, the energy efficiency of both AOP methods employed during this study are assessed.

Materials and Methods

Pharmaceutical Compounds

Acetaminophen (Acros Organics; CAS #103-92-2; purity: 98%), atenolol (Acros Organics; CAS #29122-68-7; purity: 98%), 17a-ethynyl estradiol (Acros Organics; CAS #57-63-6; purity: 98%), ibuprofen (Acros Organics; CAS #15687-27-1; purity: 99%), naproxen (MP Biomedicals; CAS #22204-53-1; purity: 99%), and sulfamethoxazole (MP Biomedicals; CAS #723-46-6; purity: 99%) were used to prepare a 400 mg/L pharmaceutical cocktail in 25 mL of methanol (Certified ACS; Fisher Scientific; CAS #67-56-1; purity: 99.9%). Pharmaceutical physicochemical parameters are found in Table S1. The pharmaceutical cocktail was stored in a -20°C freezer in between experiments. Acetaminophen-d3, atenolol-d7, estradiol-2,4,6,16,16-d4, (S)-(+)-ibuprofen-d3, (S)-naproxen-d3, sulfamethoxazole-d4 were all purchased from Toronto Research Chemicals. These deuterated standards were used to create a separate 10 mg/L super stock in 25 mL of methanol. The deuterated standard super stock was also stored in a -20°C freezer in between experiments.

UV/H_2O_2 Experiments

The UV/H_2O_2 experiments were carried out with six pharmaceuticals in nanopure water, synthetic fresh urine, and synthetic hydrolyzed urine. The synthetic urine recipes for both fresh and hydrolyzed urine are provided in Table S2 and are based on previous studies.(33,34) Experimental solutions in nanopure water or the synthetic urines were prepared by spiking the

pharmaceutical cocktail stocks to achieve concentrations of 1 mg/L and H_2O_2 (Fisher Chemical; CAS #7722-81-1) stocks to achieve a concentration of 20 mg/L. Prior to treatment, initial samples (1.41 mL) were removed from the beaker reactors and placed in 2 mL screw top vials. The experimental solutions were exposed to a low-pressure ultraviolet lamp at a fluence rate of 0.54 mW/cm^2 (Phillips Inc. #TUV PL-S 13W/2P) in a standard fluorescent light fixture with constant stirring. Every 2.5 minutes, aliquots were collected from the reactors and placed in 2 mL screw top vials. All samples were spiked with 0.09 mL of the 10 mg/L deuterated internal standard stock. Samples were collected up to a total reaction time of 20 minutes for nanopure water solutions and up to 60 minutes for synthetic urine solutions. This results in a fluence dose of 650 mJ/cm^2 and 1,900 mJ/cm^2 for the nanopure water and synthetic urine solutions, respectively.

Plasma Experiments

The plasma reactor consisted of a 22-gauge, stainless-steel, high voltage electrode (McMaster-Carr) fed into cylindrical quartz tubing (Quartz Scientific) which acted as the dielectric barrier (Figure S1). The ground electrode was a corrosion-resistant tungsten wire (McMaster-Carr) wrapped around the quartz tubing. Argon gas was fed into the tubing at a rate of about 2.126 L min^{-1} controlled by a 150-mm correlated flowmeter (Cole-Palmer). Power was supplied by a neon transformer (Franceformer; Fairview, Tennessee) with an output voltage of 15,000 volts and a frequency of 60 Hz.

Similar to the UV/H_2O_2 experiments, experimental solutions consisted of nanopure water, synthetic fresh urine, or synthetic hydrolyzed urine spiked with the six pharmaceuticals to achieve 1 mg/L. The experimental solution (72 mL) was transferred to a 100 mL graduated cylinder. At time = 0, an initial aliquot (1.41 mL) was collected from the reactor, placed in a 2 mL screw top

vial, and spiked with 0.09 mL of the deuterated standard. During treatment with the plasma reactor, aliquots were collected from the experimental solutions every 2.5 minutes for up to 20 minutes and were spiked with the deuterated internal standard stocks.

Analytical Methods

Pharmaceuticals in treated samples were quantified through online solid-phase extraction (SPE) followed by high performance liquid chromatography (HPLC) and high-resolution mass spectrometry (HRMS). Standard curves were prepared and consisted of six calibration points ranging from 100 mg/L to 1,200 mg/L and each containing 600 mg/L of the deuterated internal standard. Each standard curve was considered successful if the R^2 was greater than 0.99. Online SPE was conducted with the Thermo Scientific Equan setup and a Hypersil Gold aQ trapping column (20 x 2.1 mm, 12 μM particle size; Thermo Fisher Scientific). An Accucore aQ column (50 x 2.1 mm, 2.6 μm particle size; Thermo Fisher Scientific) was used for chromatographic separation with an injection volume of 1000 mL into the trapping column. To elute the selected pharmaceuticals from the column with minimal interference two mobile phases were applied in gradient flow consisting of nanopure water and 0.1% formic acid for mobile phase A and methanol and 0.1% formic acid for mobile phase B. The flow rate was 0.175 mL/min for 12 minutes of the gradient flow and increased to 0.25 mL/min over the course of 0.2 minutes and held for 1.8 minutes. Finally, the flow rate was decreased from 0.25 to 0.175 mL/min over the course of 0.2 minutes. The mobile phase gradient flow was as follows: mobile phase A was held at 90% for 3 minutes, steadily increased to 90% mobile phase B over the course of 8 minutes, held at 90% mobile phase B for 1 minute, and finally returned to 90% mobile phase A over 0.2 minutes.

All six pharmaceuticals were ionized in positive mode through electron spray ionization. Source parameters included: capillary temperature of 250 °C, auxiliary gas heater temperature of 275 °C, a spray voltage of 3.5 kV, sheath gas flow rate of 30 arbitrary units, auxiliary gas flow rate of 20 arbitrary units, and sweep gas flow rate of 1 arbitrary unit. Resolution was set at 70,000 with a target automatic gain control (AGC) of 1 x 10^{-6} and a scan range from 150 to 2000 m/z. Analytes and their respective deuterated forms were found through their retention times and exact mass (Table S3). Concentrations for the treated samples were quantified by comparing the response ratio (the area of the target analyte divided by the area of the deuterated standard) of the samples to that of the standard curves generated.

Data Analysis

Observed rate constants for each pharmaceutical in both reactor systems were determined by assuming pseudo-first order conditions. Reported k_{obs} values in all matrixes were determined based on the slopes found in Figures S2-S4 and are reported in Table S4. In the case of the UV/H_2O_2, the reaction mechanism includes both direct and indirect photolysis and is defined as follows:

$$\frac{d[Pharm]}{dt} = -k_{d,Pharm}[Pharm] - k_{\cdot OH,Pharm}[\cdot OH][Pharm]$$

$$= -k_{obs}^{UV}[Pharm]$$

where $k_{d,Pharm}$ (s^{-1}) is the direct photolysis rate constant, $k_{\times OH,Pharm}$ ($M^{-1}s^{-1}$) is the second-order rate constant with hydroxyl radical, k_{obs}^{UV} (s^{-1}) is the observed rate constant, [Pharm] (M) is the pharmaceutical concentration, and [×OH] (M) is the hydroxyl radical concentration. Integrating results in the relationship:

$$ln\left(\frac{[Pharm]}{[Pharm]_o}\right) = -k_{obs}^{UV}t\ .$$

The observed rate constant can be determined by plotting the experimentally determined pharmaceutical concentration ratio over time. For the case of the plasma reactor, the observed rate constant is defined as:

$$\frac{d[Pharm]}{dt} = -k_{\cdot OH,Pharm}[\cdot OH][Pharm] - k_{o_3,Pharm}[O_3][Pharm] - k_{d,Pharm}[Pharm] - \cdots$$

$$= -k_{obs}^{P}[Pharm]$$

$$ln\left(\frac{[Pharm]}{[Pharm]_o}\right) = -k_{obs}^{P}t \ .$$

Statistical analysis of observed rate constants was conducted using GraphPad Prism version 8.4.3 for MacOS Catalina, GraphPad Software, San Diego, California USA, www.graphpad.com.

Energy Efficiency Calculations

E_{EO} is a metric defined by Bolton et al.(35) that indicates the energy investment required to achieve 90% removal of a contaminant. E_{EO} is calculated for an idealized batch reactor as follows:

$$E_{EO} = \frac{38.38\ P}{V\ k}$$

where P is the power (kW), V is the volume (L), and k is the observed rate constant (min^{-1}). An individual E_{EO} was calculated using each of the observed rate constants of the target pharmaceuticals treated in each of the reactors across all three experimental matrices.

The UV irradiance of our UV/H_2O_2 reactor setup was determined by potassium iodide actinometry as described previously(36) and was used as the power value for the E_{EO} calculation. We measured the power used by the plasma reactor to degrade the pharmaceuticals by measuring

188 the voltage and current running through the positive and ground electrodes described above. The
189 voltage was measured using a high voltage probe (Tektronix P6015A; Beaverton, Oregon) and the
190 current was measured with a Pearson coil. The signals from the probe and coil were monitored and
191 captured through a BK Precision Model-2190D oscilloscope (Yorba Linda, California). These
192 signals were then integrated over a single phase to determine the power dissipated directly into the
193 reactor.
194
195 **Results and Discussion**
196 **Hydroxyl radicals are the primary degradation mechanism in plasma treatment**
197 Experiments with nanopure water show that the UV/H_2O_2 reactor transforms our test
198 pharmaceuticals in a similar manner to other UV/H_2O_2 studies in water. Sulfamethoxazole, which
199 has a higher quantum yield and molar extinction coefficient than the other pharmaceuticals and is
200 thus susceptible to both direct and indirect photolysis, had a rate constant between 20 and 65 times
201 higher than all the other pharmaceuticals tested (Figure 1) and this difference was significant
202 (Tukey's multiple comparison test, $p < 0.05$). This pattern is similar to what was found by Wols et
203 al. 2013 in which sulfamethoxazole degraded more rapidly than acetaminophen and atenolol at a
204 comparable UV dose and H_2O_2 concentration.(37) This result shows that our UV/H_2O_2
205 experimental setup produces results consistent with other published studies. We treated the same
206 set of pharmaceuticals with our experimental plasma reactor and found observed rate constants
207 ranging from 4.95×10^{-4} to 1.46×10^{-3} s^{-1}. Importantly, the observed rate constant for
208 sulfamethoxazole was within the same order of magnitude as the other pharmaceuticals tested.
209 This suggests that degradation by direct photolysis is not a significant pathway for pharmaceutical
210 loss in our plasma reactor. UV production by plasma has been reported(38); however, consistent

with our results, its contribution to the degradation of organic contaminants was negligible. Our results are also consistent with those of Singh et al. who evaluated degradation pathways for diclofenac, carbamazepine, and ciprofloxacin in a pulsed corona discharge plasma reactor and found the most prominent mechanism for mineralization was by electrophilic addition of hydroxyl radicals.(39)

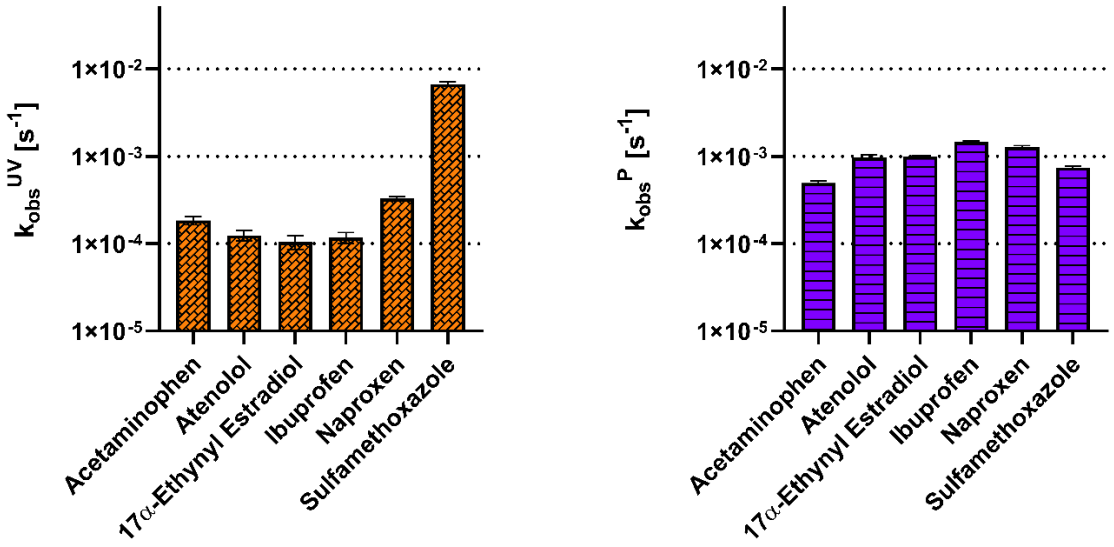

Figure 1. Observed first order rate constants for pharmaceutical loss in nanopure water treated by the UV/H_2O_2 system (left) and the plasma system (right).

Comparing the observed rate constants with reported rate constants for hydroxyl radicals, ozone, and direct photolysis confirms the conclusions from our experimental results on the impact of direct photolysis and provide insight into the contribution of ozone towards pharmaceutical degradation (Figure 2). The literature-based second-order rate constants with hydroxyl radical correspond with a higher observed rate constant for most of the pharmaceuticals. Specifically, the correlation (R^2: 0.54; significantly non-zero slope P = 0.0005) between the observed rate constants

and the hydroxyl radical second-order rate constants suggests that hydroxyl radical is the predominant oxidative agent. A lack of correlation would suggest other radical species were driving the degradation of the pharmaceuticals. By comparison, the rate constants of the ozone and UV_{254} radiation do not correlate (R^2: 0.0001 and R^2: 0.2 respectively; non-significant non-zero slope P = 0.96 and P = 0.07) with the observed rate constants (Figures S5 and S6). The larger second-order rate constants of the pharmaceuticals with hydroxyl radical demonstrate that the plasma reactor would need to generate ozone concentrations three to nine orders of magnitude greater than the hydroxyl radical concentrations to play a role in pharmaceutical degradation. The exception to this observation is with 17a-ethynyl estradiol, which has a second-order rate constant with ozone (7.4×10^9 $M^{-1}s^{-1}$) similar to the second-order rate constant with hydroxyl radical (9.8×10^9 $M^{-1}s^{-1}$). The general trend suggest that ozone is produced at insufficient quantities to increase the observed rate constant.

Our results suggest the main mechanism responsible for pharmaceutical losses observed during our plasma experiments is hydroxyl radical oxidation. However, our results do not exclude the possibility that UV and reactive species beyond hydroxyl radicals were produced; rather, they show that they were not formed at intensities sufficient to compete with hydroxyl radicals for degradation of the pharmaceutical compounds we evaluated. The types and amounts of radicals produced by plasma are impacted by operating and design conditions such as carrier gas, gas flow rates, reactor geometry, input power, type of power supply, and electrode types.(40) By making changes to these conditions, it is feasible that the primary reaction mechanism could shift to other radicals beyond hydroxyl radical, such as UV, ozone, or peroxide. However, our reactor allows us to focus on hydroxyl radical as an oxidative mechanism, which is known to be a major oxidative radical for degradation of pharmaceutical compounds.

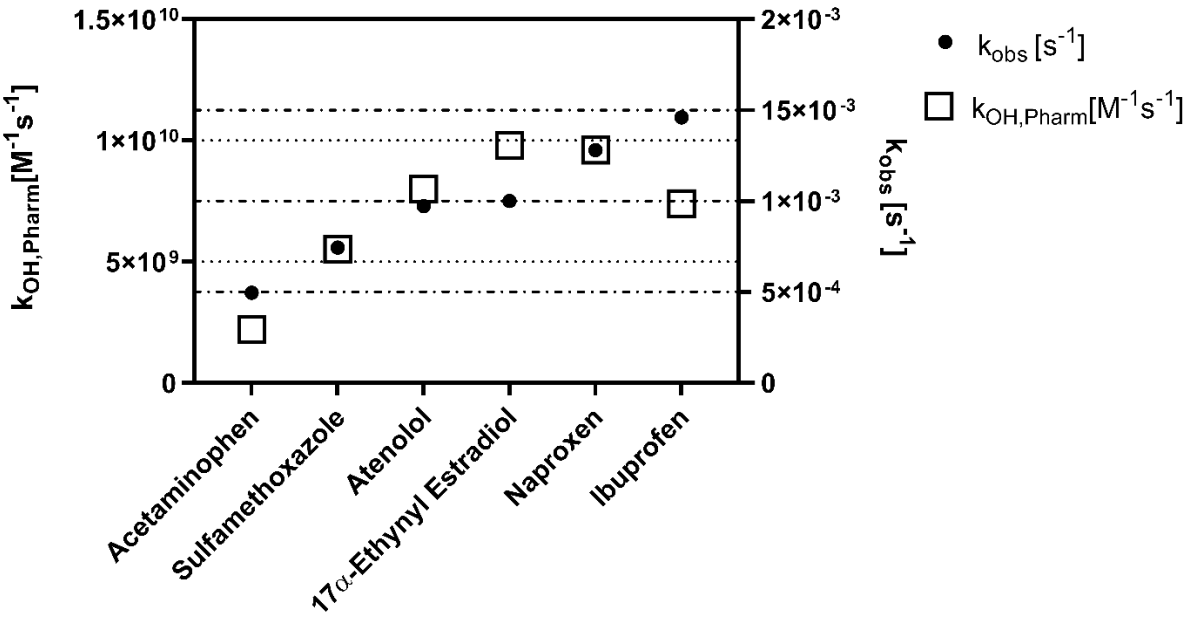

Figure 2. Second-order rate constants reported in the literature for each pharmaceutical with hydroxyl radical are presented on the left y-axis.(41–44) Observed first-order rate constants for each pharmaceutical in nanopure water are presented on the right y-axis. Both axes are presented on a linear scale to see the relationship between first and second-order rate constants.

Plasma oxidation treatment is consistent across different synthetic urine matrices

Experiments were conducted to determine if the matrix of synthetic urine would equally impact the performance of the two AOP treatments. We use a matrix performance ratio ($k_{obs,nanopure\ water}/k_{obs,synthetic\ urine}$) to characterize these matrix effects for both fresh and hydrolyzed synthetic urine; a ratio greater than one indicates that the pharmaceutical degraded faster in the nanopure water and a ratio less than one indicates degradation occurred faster in the synthetic urine (Fig. 3). Using this metric, we show that both the UV/H_2O_2 and plasma reactors were negatively impacted by the switch to a hydrolyzed synthetic urine matrix.

The hydrolyzed urine matrix introduces hydroxyl radical scavenging effects for both oxidation technologies, however to a different degree. For UV/H_2O_2 in hydrolyzed synthetic urine, the

matrix performance ratio ranged from 0.21 ± 0.030 to 5.2 ± 0.010 across all pharmaceuticals (Fig. 3a). Atenolol, ibuprofen, naproxen, and sulfamethoxazole had a ratio above one, indicating that the presence of hydroxyl radical scavengers in the urine matrix diminish the rate at which the pharmaceuticals are degraded.(34) Acetaminophen and 17α-ethynyl estradiol had matrix performance ratios below one, indicating a matrix enhancement effect. Studies have shown that the presence of bicarbonate, a compound found in hydrolyzed urine, leads to the formation of carbonate radicals in UV-AOP systems, which in turn increases the degradation rates of acetaminophen and estrogenic compounds and could explain this matrix enhancement effect.(45,46) Similarly, all of the pharmaceuticals degraded faster in nanopure water compared to hydrolyzed synthetic urine when treated with plasma (Fig. 3a). The matrix performance ratios ranged from 1.9 ± 0.010 to 9.7 ± 3.9, demonstrating a slightly greater scavenging impact with plasma treatment compared to UV/H_2O_2 treatment. For both UV/H_2O_2 AOP and plasma AOP, the hydroxyl scavengers in the hydrolyzed synthetic urine, including ammonium and bicarbonate, decrease the number of hydroxyl radicals available for the target compounds. (34) An additional effect of the plasma reactor is that the strong electric field is diminished as the conductivity of the solution increased.(47) Alternative plasma reactor configurations may lessen the negative conductivity effects. For example, an over-the-liquid plasma, which generates electrical discharges just above the water, demonstrated increased radical production at higher conductivities.(48) Use of a power supply with less time between low to high voltage (rise time)(48) could also minimize conductivity effects, as shown by Wang et al.(49)

When tested in nanopore water versus fresh synthetic urine, the UV/H_2O_2 reactor exhibited matrix performance ratios that ranged from 20 ± 4.0 to 50 ± 3.1 (Fig. 3b). Performance for the plasma reactor was less impacted by the switch to fresh synthetic urine than was UV/H_2O_2, as

290 reflected by the pharmaceuticals having matrix performance ratios ranging from 2.7 ± 0.1 to 12 ±
291 2.0 (Fig. 3b). These matrix performance ratios are similar to those observed for the plasma reactor
292 in hydrolyzed urine compared to nanopure water. The presence of creatinine at 9.7 mM (a waste
293 product released by muscles) in the fresh synthetic urine likely caused performance of the
294 UV/H_2O_2 reactor to diminish. Creatinine has a high experimental molar extinction coefficient (e =
295 246 m^2 mol^{-1}) than H_2O_2 (e = 1.86 m^2 mol^{-1}), consistent with the hypothesis that creatinine
296 interfered with H_2O_2 absorption of UV_{254}.(50) Less H_2O_2 absorption results in reduced production
297 of hydroxyl radicals. Since creatinine undergoes hydrolysis as a result of the urease enzyme
298 converting urea from urine into ammonium, creatinine is not added to the hydrolyzed synthetic
299 urine recipe.(51) The presence of different scavengers in a given matrix is key when deciding
300 which technology to use in a given urine treatment process train. Our results show that while the
301 plasma treatment efficiency is more impacted by the hydrolyzed urine constituents than the
302 UV/H_2O_2 reactor, it performed similarly (within an order of magnitude) across multiple urine
303 matrices.

304 Conductivity differences between the two urine matrices did not seem to play a significant
305 role in performance of the plasma. The conductivity of the fresh synthetic urine (16 mS/cm) was
306 less than half that of the hydrolyzed synthetic urine (36 mS/cm), and both match conductivities
307 observed for real fresh and hydrolyzed urine. Nevertheless, conductivity still played a role given
308 that switching from nanopure water (< 100 μS/cm) to synthetic urine diminished performance.
309 Shih et al. operated a point-to-plane in water plasma reactor and found that the production of
310 hydroxyl radicals diminished as the conductivity increased; however, this effect plateaued after
311 reaching 0.30 mS/cm.(47) Given that the conductivities of both synthetic urines are well above
312 this level, the negative effects of conductivity could have reached their limit.

When plasma reactors are used to degrade pharmaceuticals in complex matrices, experiments should be designed to avoid the two-fold problem of conductivity and scavenging. Guo et al. combined pulsed discharge plasma with reduced graphene oxide/TiO_2 nanocomposites to enhance the degradation potential of flumequine (fluoroquinolone antibiotic) for water treatment.(52) The reduced graphene/TiO_2 nanocomposites facilitated the formation of ozone, which ultimately led to the formation of a higher quantity of hydroxyl radicals compared to the plasma alone or the TiO_2 alone. By coupling plasma with other existing technologies, the scavengers that lower hydroxyl radical production could be counteracted and offer new degradation pathways to address pharmaceutical concerns.

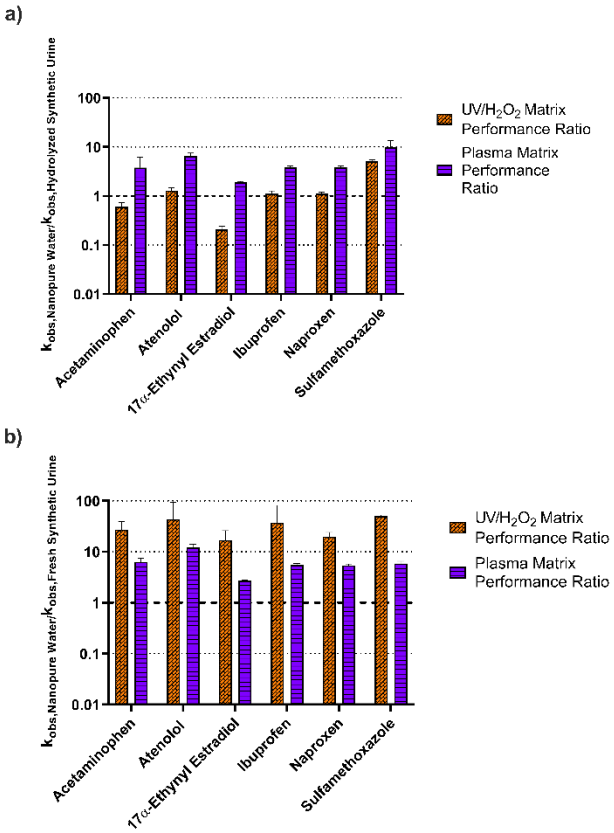

Figure 3: (a) Comparison of hydrolyzed synthetic urine matrix effects on the degradation rate of pharmaceuticals in each of the two reactors. (b) Comparison of fresh synthetic urine matrix effects on the degradation rate of pharmaceuticals in each of the two reactors.

Energy efficiency limits the scale of plasma treatment

The electric energy per order of magnitude (E_{EO}) was calculated to compare the energy intensity of the two reactors, which had different pharmaceutical degradation mechanisms, geometries, and levels of power applied. In all matrices, the E_{EO} for the UV/H_2O_2 reactor was two to three orders of magnitude smaller than the plasma reactor (Figure 4), signifying overall better energy efficiency in the UV/H_2O_2 reactor. Even in the fresh synthetic urine matrix, which reduced the removal of pharmaceuticals significantly for the UV/H_2O_2 reactor compared to nanopure water, the E_{EO} remained lower than that of the plasma reactor. Miklos et al. conducted an extensive review on several studies that evaluated the degradation of organic compounds with various technologies and found that UV/H_2O_2 was an order of magnitude more efficient than plasma.(53) Notably, these studies did not examine complex matrixes such as urine with much higher conductivities.

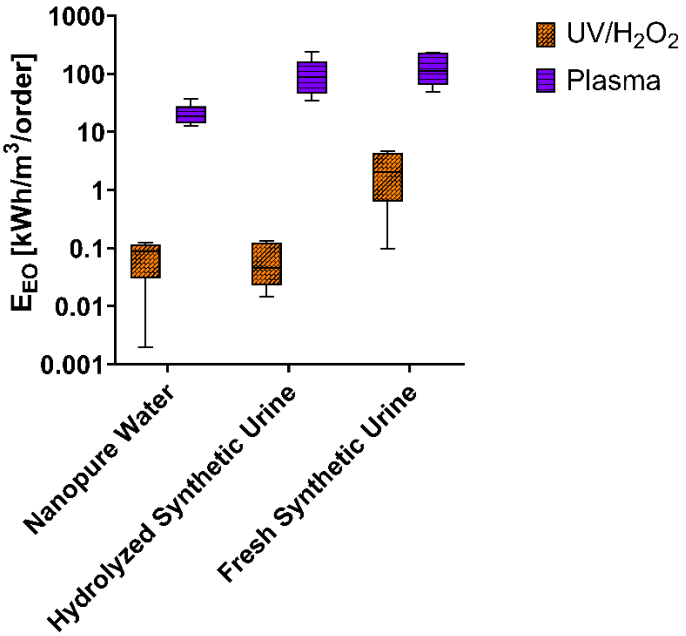

Figure 4: Calculated electric energy per order (E_{EO}) (kWh/m^3/order) for both bench-scale reactors in the nanopure water and synthetic urine matrixes. The box and whisker plot displays 95% confidence intervals for E_{EO} values (n=6, all pharmaceutical compounds in each data point).

From an energy perspective, plasma at a full scale is mainly hindered by mass transfer limitations for the dissolution of oxidative species in solution, which lower the overall process efficiency.(54) However, plasma treatment has been implemented widely in small- and medium-scale applications.(55–60) Despite plasma's lower energy efficiency per unit of treatment, plasma warrants further evaluation for possible application in resource recovery fluids such as a small-scale or on-site urine-derived fertilizer processing facilities.

Conclusions

Creating sustainable and publicly acceptable fertilizers from source-separated urine requires mitigating the release of micropollutants.(61) In this study, we compared two advanced oxidation methods to reduce pharmaceutical concentrations in urine. Our results show that a dielectric barrier discharge plasma reactor can oxidize pharmaceuticals in both fresh and hydrolyzed synthetic urine; however, it did so at a higher energy cost than UV/H_2O_2, which is an established technology that has many large-scale deployments. Collection and production of urine-derived fertilizers can occur at various scales, including the building-scale that has single- or multiple- dwelling units or multi-floor office buildings. Plasma oxidation has the benefit of chemical-free implementation and should be considered as an option, along with other traditional advanced oxidation processes, for building-scale pharmaceutical degradation at the point of urine collection and processing. Furthermore, the wide range of plasma reactor geometries could allow for treatment-specific configurations. Despite the lack of evidence for the role of reactive chemical species beyond the hydroxyl radical in the reactor configuration evaluated for this study, changes to the reactor geometry, carrier gas, power supply used, and various other operating parameters could be implemented to improve the efficiency of pharmaceutical treatment in urine-derived fertilizers. Alternatively, the reactor can be optimized to produce and transfer more hydroxyl

radicals than seen in our study, which would enhance their diffusion into the liquid phase. Some intermediate liquids formed during urine processing that capture the pharmaceuticals, such as the residual water produced during phosphorus-capturing struvite precipitation(62), may be more amenable to plasma treatment than unprocessed urine. Finally, pharmaceutical degradation mechanisms and pathways due to plasma treatment can be further elucidated by studying the transformation products of treated pharmaceuticals.

Conflicts of Interest

There are no conflicts of interest to declare.

Acknowledgements

This research was supported by the U.S. National Science Foundation under award number INFEWS 1639244. The authors would like to thank Drs. Selman Mujovic, John Foster, Tian Xia, and Herek Clack for their guidance in construction and operation of the plasma reactor.

References

1. EPA US. Biological Nutrient Removal Processes and Costs. 2007.
2. Maurer M, Schwegler P, Larsen TA. Nutrients in urine: energetic aspects of removal and recovery. Water Sci Technol [Internet]. 2003 Jul 1;48(1):37 LP – 46. Available from: http://wst.iwaponline.com/content/48/1/37.abstract
3. Cordell D, White S. Peak phosphorus: Clarifying the key issues of a vigorous debate about long-term phosphorus security. Sustainability. 2011;3(10):2027–49.
4. Udert KM, Larsen TA, Gujer W. Fate of major compounds in source-separated urine. Water Sci Technol. 2006;54(11–12):413–20.
5. Larsen TA, Alder AC, Eggen RIL, Maurer M, Lienert J. Source separation: Will we see a paradigm shift in wastewater handling? Environ Sci Technol. 2009;43(16):6121–5.
6. Hilton SP, Keoleian GA, Daigger GT, Zhou B, Love NG. Life Cycle Assessment of Urine Diversion and Conversion to Fertilizer Products at the City Scale. Environ Sci Technol [Internet]. 2020; Available from: http://journals.sagepub.com/doi/10.1177/1120700020921110%0Ahttps://doi.org/10.1016/j.reuma.2018.06.001%0Ahttps://doi.org/10.1016/j.arth.2018.03.044%0Ahttps://reader.elsevier.com/reader/sd/pii/S1063458420300078?token=C039B8B13922A2079230DC9AF11A333E295FCD8
7. Lienert J, Bürki T, Escher BI. Reducing micropollutants with source control: Substance flow analysis of 212 pharmaceuticals in faeces and urine. Water Sci Technol. 2007;56(5):87–96.
8. Deo RP. Pharmaceuticals in the Surface Water of the USA: A Review. Curr Environ Heal Reports. 2014;1(2):113–22.

9. Zhang R, Yang Y, Huang CH, Zhao L, Sun P. Kinetics and modeling of sulfonamide antibiotic degradation in wastewater and human urine by UV/H 2 O 2 and UV/PDS. Water Res [Internet]. 2016;103:283–92. Available from: http://dx.doi.org/10.1016/j.watres.2016.07.037

10. Zhang R, Yang Y, Huang CH, Li N, Liu H, Zhao L, et al. UV/H2O2 and UV/PDS Treatment of Trimethoprim and Sulfamethoxazole in Synthetic Human Urine: Transformation Products and Toxicity. Environ Sci Technol. 2016;50(5):2573–83.

11. Köpping I, McArdell CS, Borowska E, Böhler MA, Udert KM. Removal of pharmaceuticals from nitrified urine by adsorption on granular activated carbon. Water Res X. 2020;9.

12. Ikehata K, Jodeiri Naghashkar N, Gamal El-Din M. Degradation of aqueous pharmaceuticals by ozonation and advanced oxidation processes: A review. Ozone Sci Eng. 2006;28(6):353–414.

13. Feng L, van Hullebusch ED, Rodrigo MA, Esposito G, Oturan MA. Removal of residual anti-inflammatory and analgesic pharmaceuticals from aqueous systems by electrochemical advanced oxidation processes. A review. Chem Eng J. 2013;228:944–64.

14. Lester Y, Avisar D, Gozlan I, Mamane H. Removal of pharmaceuticals using combination of UV/H2O 2/O3 advanced oxidation process. Water Sci Technol. 2011;64(11):2230–8.

15. Klavarioti M, Mantzavinos D, Kassinos D. Removal of residual pharmaceuticals from aqueous systems by advanced oxidation processes. Environ Int [Internet]. 2009;35(2):402–17. Available from: http://dx.doi.org/10.1016/j.envint.2008.07.009

16. Sirés I, Brillas E, Oturan MA, Rodrigo MA, Panizza M. Electrochemical advanced oxidation processes: Today and tomorrow. A review. Environ Sci Pollut Res.

2014;21(14):8336–67.

17. Kwon BG, Ryu S, Yoon J. Determination of hydroxyl radical rate constants in a continuous flow system using competition kinetics. J Ind Eng Chem. 2009;15(6):809–12.

18. Haag WR, David Yao CC. Rate Constants for Reaction of Hydroxyl Radicals with Several Drinking Water Contaminants. Environ Sci Technol. 1992;26(5):1005–13.

19. Anpilov a M, Barkhudarov EM, Bark YB, Zadiraka Y V, Christofi M, Kozlov YN, et al. Electric discharge in water as a source of UV radiation, ozone and hydrogen peroxide. J Phys D Appl Phys. 2001;34:993–9.

20. Bruggeman P, Schram DC. On OH production in water containing atmospheric pressure plasmas. Plasma Sources Sci Technol. 2010;19(4).

21. Lukes P, Appleton AT, Locke BR. Hydrogen Peroxide and Ozone Formation in Hybrid Gas–Liquid Electrical Discharge Reactors. IEEE Trans Ind Appl. 2004;40(1):60–7.

22. Sunka P, Babický V, Clupek M, Lukes P, Simek M, Schmidt J, et al. Generation of chemically active species by electrical discharges in water. Plasma Sources Sci Technol. 1999;8(2):258–65.

23. Velikonja J, Bergougnou MA, Castle GSP, Caims WL, Inculet II. Co-generation of ozone and hydrogen peroxide by dielectric barrier AC discharge in humid oxygen. Ozone Sci Eng. 2001;23(6):467–78.

24. Joshi RP, Thagard SM. Streamer-like electrical discharges in water: Part I. fundamental mechanisms. Plasma Chem Plasma Process. 2013;33(1):1–15.

25. Joshi RP, Thagard SM. Streamer-like electrical discharges in water: Part II. environmental applications. Plasma Chem Plasma Process. 2013;33(1):17–49.

26. Locke BR, Sato M, Sunka P, Hoffmann MR, Chang JS. Electrohydraulic discharge and

452 nonthermal plasma for water treatment. Ind Eng Chem Res. 2006;45(3):882–905.
453 27. Liu F, Sun P, Bai N, Tian Y, Zhou H, Wei S, et al. Inactivation of bacteria in an aqueous
454 environment by a direct-current, cold-atmospheric-pressure air plasma microjet. Plasma
455 Process Polym. 2010;7(3–4):231–6.
456 28. Kornev I, Osokin G, Galanov A, Yavorovskiy N, Preis S. Formation of Nitrite- and
457 Nitrate-Ions in Aqueous Solutions Treated with Pulsed Electric Discharges. Ozone Sci
458 Eng. 2013;35(1):22–30.
459 29. Foster JE, Adamovsky G, Gucker SN, Blankson IM. A comparative study of the time-
460 resolved decomposition of methylene blue dye under the action of a nanosecond
461 repetitively pulsed dbd plasma jet using liquid chromatography and spectrophotometry.
462 IEEE Trans Plasma Sci. 2013;41(3):503–12.
463 30. Malik MA, Ubaid-Ur-Rehman, Ghaffar A, Ahmed K. Synergistic effect of pulsed corona
464 discharges and ozonation on decolourization of methylene blue in water. Plasma Sources
465 Sci Technol. 2002;11(3):236–40.
466 31. Gao J, Wang X, Hu Z, Deng H, Hou J, Lu X, et al. Plasma degradation of dyes in water
467 with contact glow discharge electrolysis. Water Res. 2003;37(2):267–72.
468 32. Sugiarto AT, Ito S, Ohshima T, Sato M, Skalny JD. Oxidative decoloration of dyes by
469 pulsed discharge plasma in water. J Electrostat. 2003;58(1–2):135–45.
470 33. Tilley E, Atwater J, Mavinic D. Effects of storage on phosphorus recovery from urine.
471 Environ Technol. 2008;29(7):807–16.
472 34. Zhang R, Sun P, Boyer TH, Zhao L, Huang CH. Degradation of pharmaceuticals and
473 metabolite in synthetic human urine by UV, UV/H2O2, and UV/PDS. Environ Sci
474 Technol. 2015;49(5):3056–66.

35. Bolton JR, Stefan MI. Fundamental photochemical approach to the concepts of fluence (UV dose) and electrical energy efficiency in photochemical degradation reactions. Res Chem Intermed. 2002;28(7–9):857–70.
36. Rahn R. Potassium Iodide as a Chemical Actinometer for 254 nm Radiation : Use of Iodate as an Electron Scavenger. Photochem Photobiol. 1997;66(4):450–5.
37. Wols BA, Hofman-Caris CHM, Harmsen DJH, Beerendonk EF. Degradation of 40 selected pharmaceuticals by UV/H2O2. Water Res [Internet]. 2013;47(15):5876–88. Available from: http://dx.doi.org/10.1016/j.watres.2013.07.008
38. Huang HB, Ye DQ, Fu ML, Feng F Da. Contribution of UV light to the decomposition of toluene in dielectric barrier discharge plasma/photocatalysis system. Plasma Chem Plasma Process. 2007;27(5):577–88.
39. Singh RK, Philip L, Ramanujam S. Rapid degradation, mineralization and detoxification of pharmaceutically active compounds in aqueous solution during pulsed corona discharge treatment. Water Res [Internet]. 2017;121:20–36. Available from: http://dx.doi.org/10.1016/j.watres.2017.05.006
40. Locke BR, Thagard SM. Analysis and review of chemical reactions and transport processes in pulsed electrical discharge plasma formed directly in liquid water. Plasma Chem Plasma Process. 2012;32(5):875–917.
41. Andreozzi R, Caprio V, Marotta R, Radovnikovic A. Ozonation and H 2 O 2/UV treatment of clofibric acid in water: a kinetic investigation. J Hazard Mater. 2003;103(3):233–46.
42. Benner J, Salhi E, Ternes T, von Gunten U. Ozonation of reverse osmosis concentrate: Kinetics and efficiency of beta blocker oxidation. Water Res. 2008;42(12):3003–12.

43. Huber MM, Canonica S, Park GY, Von Gunten U. Oxidation of pharmaceuticals during ozonation and advanced oxidation processes. Environ Sci Technol. 2003;37(5):1016–24.
44. Packer JL, Werner JJ, Latch DE, McNeill K, Arnold WA. Photochemical fate of pharmaceuticals in the environment: Naproxen, diclofenac, clofibric acid, and ibuprofen. Aquat Sci. 2003;65(4):342–51.
45. Bai Y, Cui Z, Su R, Qu K. Influence of DOM components, salinity, pH, nitrate, and bicarbonate on the indirect photodegradation of acetaminophen in simulated coastal waters. Chemosphere [Internet]. 2018;205:108–17. Available from: https://doi.org/10.1016/j.chemosphere.2018.04.087
46. Lian L, Miao C, Hao Z, Liu Q, Liu Y, Song W, et al. Reevaluation of the contributions of reactive intermediates to the photochemical transformation of 17β-estradiol in sewage effluent. Water Res [Internet]. 2021;189:116633. Available from: https://doi.org/10.1016/j.watres.2020.116633
47. Shih KY, Locke BR. Optical and electrical diagnostics of the effects of conductivity on liquid phase electrical discharge. IEEE Trans Plasma Sci. 2011;39(3):883–92.
48. Thagard SM, Takashima K, Mizuno A. Chemistry of the positive and negative electrical discharges formed in liquid water and above a gas-liquid surface. Plasma Chem Plasma Process. 2009;29(6):455–73.
49. Xie X, Wang Z, Li Y, Zhan L, Nie Z. Investigation and Applications of In-Source Oxidation in Liquid Sampling-Atmospheric Pressure Afterglow Microplasma Ionization (LS-APAG) Source. J Am Soc Mass Spectrom. 2017;28(6):1036–47.
50. BŁedzka D, Gryglik D, Olak M, Gebicki JL, Miller JS. Degradation of n-butylparaben and 4-tert-octylphenol in H2O2/UV system. Radiat Phys Chem. 2010;79(4):409–16.

51. Miller TJ. The kinetics and mechanism of the hydrolysis of creatinine in urine. Anal Lett. 1991;24(10):1779–84.
52. Guo H, Jiang N, Wang H, Shang K, Lu N, Li J, et al. Degradation of flumequine in water by pulsed discharge plasma coupled with reduced graphene oxide/TiO2 nanocomposites. Sep Purif Technol. 2019;218(March):206–16.
53. Miklos DB, Remy C, Jekel M, Linden KG, Drewes JE, Hübner U. Evaluation of advanced oxidation processes for water and wastewater treatment – A critical review. Water Res. 2018;139:118–31.
54. Wardenier N, Liu Z, Nikiforov A, Van Hulle SWH, Leys C. Micropollutant elimination by O3, UV and plasma-based AOPs: An evaluation of treatment and energy costs. Chemosphere [Internet]. 2019;234:715–24. Available from: https://linkinghub.elsevier.com/retrieve/pii/S0045653519312627
55. Foster JE, Weatherford B, Gillman E, Yee B. Underwater operation of a DBD plasma jet. Plasma Sources Sci Technol. 2010;19(2).
56. Gerrity D, Stanford BD, Trenholm RA, Snyder SA. An evaluation of a pilot-scale nonthermal plasma advanced oxidation process for trace organic compound degradation. Water Res [Internet]. 2010;44(2):493–504. Available from: http://dx.doi.org/10.1016/j.watres.2009.09.029
57. Kim KS, Yang CS, Mok YS. Degradation of veterinary antibiotics by dielectric barrier discharge plasma. Chem Eng J [Internet]. 2013;219:19–27. Available from: http://dx.doi.org/10.1016/j.cej.2012.12.079
58. Magureanu M, Piroi D, Mandache NB, David V, Medvedovici A, Bradu C, et al. Degradation of antibiotics in water by non-thermal plasma treatment. Water Res.

2011;45(11):3407–16.

59. Mok YS, Jo JO, Lee HJ, Ahn HT, Kim JT. Application of dielectric barrier discharge reactor immersed in wastewater to the oxidative degradation of organic contaminant. Plasma Chem Plasma Process. 2007;27(1):51–64.

60. Stará Z, Krčma F, Nejezchleb M, Dušan Skalný J. Organic dye decomposition by DC diaphragm discharge in water: Effect of solution properties on dye removal. Desalination. 2009;239(1–3):283–94.

61. Segrè Cohen A, Love NG, Nace KK, Árvai J. Consumers' Acceptance of Agricultural Fertilizers Derived from Diverted and Recycled Human Urine. Environ Sci Technol. 2020;54(8):5297–305.

62. Ronteltap M, Maurer M, Gujer W. The behaviour of pharmaceuticals and heavy metals during struvite precipitation in urine. Water Res. 2007;41(9):1859–68.